Journal of Asian Earth Sciences xxx (xxxx) xxx–xxx

Contents lists available at ScienceDirect

Journal of Asian Earth Sciences

journal homepage: www.elsevier.com/locate/jseaes

Full length article

Influence of water on granite generation: Modeling and perspective

Xin Chen[a,b], Cin-Ty A. Lee[b], Xiao-Lei Wang[a,*], Ming Tang[b]

[a] State Key Laboratory for Mineral Deposits Research, School of Earth Sciences and Engineering, Nanjing University, Nanjing 210023, China
[b] Department of Earth Sciences, Rice University, Houston, TX 77005, USA

ARTICLE INFO

Keywords:
Water content
Granitic rock
Hygrometer
Magmatic differentiation
Modeling

ABSTRACT

Water influences the physics and chemistry of magmatic differentiation because it reduces the melting point, decreases melt viscosity, modifies phase equilibria, and controls how latent heat is released. Here, we explore how compositional trends of fractionating magmas can be used to evaluate the amount of water in the crystallizing system. Of interest is the role of water in generating silicic magmas such as granites and rhyolites. Water expands the crystallization window over which silicic melts are stable, such that granites are limited to small residual melt fractions ($F < 0.2$) under dry conditions but stable over a wider range of residual melt fractions ($F < 0.6$) at high water contents. Variations of SiO_2 versus F are relatively insensitive to oxygen fugacity and can be used as a hygrometer for granitoids, where F is estimated through relative enrichments in incompatible elements, such as Th and K. We also show that generation of granitoids in arc environments follow distinctly different Mg#-SiO_2 trends compared with anorogenic or intra-plate granites. We confirm that arc magmas differentiate at higher water contents and possibly higher oxygen fugacities than anorogenic/intra-plate magmas. Finally, Archean TTGs (tonalite, trondhjemite, and granodiorite) show similar Mg#-SiO_2 systematics as Phanerozoic arc-related granitoids, suggesting similar petrogenetic physical and chemical conditions.

1. Introduction

There is considerable controversy over how far back in time the Earth had oceans and plate tectonics (Condie, 2013; Tang et al., 2016; Valley et al., 2014; Watson and Harrison, 2005; Weller and St-Onge, 2017). Part of the controversy lies in the significance of granitic rocks in the past. For example, it is widely thought that making granites requires water (Campbell and Taylor, 1983; Lee et al., 2015; Sisson and Grove, 1993; Whitney, 1988), so the presence of granitic rocks requires subduction of hydrated oceanic crust or re-melting of hydrated crust (Annen et al., 2006; Kelley and Cottrell, 2009; Sizova et al., 2015). This view is partly based on the fact that water decreases the melting point of mafic rocks (Asimow and Langmuir, 2003; Katz et al., 2003; Wolf and Wyllie, 1994), thereby making it easier, at least energetically, to generate granites by re-melting the crust. Low temperatures recorded by Ti in Hadean to early Archean zircons have been interpreted to reflect crystallization from minimum-temperature granitic magmas, that is, at water-saturated conditions, implying the presence of water and plate tectonics (Watson and Harrison, 2005).

Interpretations of such data, however, may be more complicated. Granitic magmas can be formed from both hydrous and anhydrous magmas (Kushiro, 1972), although hydrous magmas produce more granitic magmas from the same parental mafic rocks (Lee et al., 2015; Melekhova et al., 2013). With progressive crystallization, water concentrates in the residual melt, resulting in water saturation after extreme crystallization. The residual liquids will reflect minimum-melting temperatures even though they fractionated from relatively dry parental magmas (Lee and Bachmann, 2014; Nutman, 2006). What is clear is that temperature constraints alone are not sufficient to determine whether granitoids derived from hydrous or anhydrous parents. Therefore, exploring additional ways of inferring water content is worthwhile.

Here, we show that water controls the variation of SiO_2 during magmatic differentiation because melt productivity varies as a function of bulk water content. We apply these concepts using major and trace elements to map out average water contents of various magmatic differentiation series in space and time.

2. Data compilation and modeling

2.1. Data compilation

We compiled a database of granitoids and associated mafic to intermediate rocks to explore regional magmatic differentiation in

* Corresponding author.
E-mail address: wxl@nju.edu.cm (X.-L. Wang).

https://doi.org/10.1016/j.jseaes.2018.12.001
Received 1 December 2018; Accepted 5 December 2018

Table 1
Data sources for compiled global "A type granite series".

Mantle plume/hotspot	
Emeishan LIP south China, 260–250 Ma	GEOROC (http://georoc.mpch-mainz.gwdg.de/georoc/)
Tule Basin of Northeastern Vietnam, 260–250 Ma	Our unpublished data
ELIP SW China, 260–250 Ma	Zhong et al. (2007)
White Mountain magma series of New Hampshire, USA and southern Quebec Canada (Eby, 1987), 200–165 Ma granite, 140–110 Ma bimodal basalt and rhyolite	Eby et al. (1992)
Oceanic islands from Reunion Island, Indian Ocean	Eby (1990)
Oceanic islands from Ascension Island, South Atlantic	
Younger granites of Nigeria	
Sudan suites	
MULL the British Tertiary Igneous Province (BTIP) of northwest Scotland from Attenuated crust	
Kaerven complex, East Greenland	Holm and Prægel (1988)
Velasco, Bolivia	Fletcher and Beddoe-Stephens (1987)
Rift	
Naivasha comendites, East African Rift system	Macdonald et al. (1987)
Yemen granite suite, bimodal, Yemen rift (Capaldi et al., 1987)	Capaldi et al. (1987)
Zomba-Malosa granites, Chilwa province, Malawi	Woolley and Jones (1987)
Oslo graben of southeastern Norway	Eby (1990)
Central Tianshan orogen, China	Dong et al. (2011)
Eastern Trans-Pecos magmatic province, Texas	Nelson et al. (1987)
Wenquan granite from N China Craton	Jiang et al. (2011)
Post-orogenic setting	
subalkalic-peralkalic rhyolites of the southern British Caledonides	Leat et al. (1986)
Tibetan, china	Qu et al. (2012)
Guangdong SE China, bimodal	Zhu et al. (2010)
Evisa (Corsican province)	Bonin et al. (1978)
Bega batholith of the Lachlan Fold Belt of southeastern Australia	Collins et al. (1982)
Narraburra granite, Lachland fold belt	Wormald and Price (1988)
Topsails suite of western Newfoundland	Eby (1990)
Arabian Peninsula, Precambrian	
Malani suite of North Peninsular India	
South China	Zhao et al. (2008)
(Suomenniemi complex) from Fennoscandia	Rämö (1991)
South Margin of N China Craton	Zhao and Zhou (2009)

different tectonic settings. Representative arc magma compositions were compiled from the Peninsular Ranges Batholith (PRB) in California, remnants of a Cretaceous continental arc. Intra-plate or anorogenic magma compositions were compiled from Iceland and the Snake River Plain-Yellowstone (SRPY). Global A-type (i.e., "anorogenic") granite series and associated rocks were also compiled. Data for PRB (n = 289) were from Lee et al. (2007). Data for Iceland (n = 6920) and SRPY (n = 6477) are from the GEOROC database (http://georoc.mpch-mainz.gwdg.de/georoc/). For the global "A-type granite series" and their volcanic counterparts, the data (n > 1600) were obtained from 30 regions, and were divided into three types of tectonic setting: plume/hotspot, post-orogenic, and rift settings. Detailed references are shown in Table 1.

2.2. Modeling magma differentiation

To simulate residual melt compositions during magma differentiation, we used the thermodynamic program Rhyolite-MELTS (Gualda and Ghiorso, 2015) to calculate the cooling and crystallization path assuming that all the intra-continental granitoids are generated from parental basaltic magma. Comparison based on the same criterion is straight-forward and useful to evaluate different magmatic processes. Calculations were done for closed-system batch crystallization beginning from the liquidus and cooling at 5 °C increments at constant pressures characteristic of the upper crust (< 15 km); upper crustal pressures were chosen because most granitoids have been shown to emplace at low pressures (Ague and Brimhall, 1988; Farner and Lee, 2017). Specifically, for granitoids generated in subduction zones (i.e. arc-related granitoids), we simulated crystallization of basaltic magmas at 3 kbar, which is equal to 10 km's depth (Ague and Brimhall, 1988). More exotic magmas, such as those anorogenic granitoids, likely emplaced at shallower depths. We therefore simulated magma differentiation at 1 kbar (Clemens et al., 1986). In any case, pressure does not change the tendency of the calculated curves. The effect of oxygen fugacity (fO_2) and initial water content were taken into account for each simulation, and the oxygen fugacity was buffered at the fayalite–-magnetite–quartz (ΔFMQ) buffer from 0 to +2. The starting water content varies from 0 to 4 wt%. Details of starting compositions and modeling conditions are listed in Table 2.

2.3. Extent of magma differentiation

To estimate the extent of magmatic differentiation relative to the parental magma, we estimate the integrated effective residual melt fraction F that is determined from the enrichment of a highly incompatible element in the magma (C) relative to its parent concentration C_o, $F \approx C_o/C$ (Shaw, 1970). We assume that this effective F represents the residual melt fraction formed by crystal fractionation of a cooling parental basaltic magma. If instead the magma was generated by partial melting of hydrated basalt, F would represent the effective melt fraction produced. As F decreases, incompatible elements become more enriched in the residual melt. The elements K and Th are good candidates to calculate F because they both behave almost perfectly incompatibly through most of the differentiation processes and show progressive enrichments with increasing SiO_2 (Figs. 1 and 2; Glazner and Johnson, 2013; Rollinson, 2014; Whitney, 1988). Therefore, we use the relative concentrations of K and Th to estimate the melt fraction F during magmatic differentiation in generating granitoids.

To estimate C_o for Th and K systems of arc and intra-plate magmas, we linearly regressed Th-MgO and K_2O-MgO data for regional differentiation trends and then extrapolated the regression to infer Th and K_2O concentrations at 8 wt% MgO. While magma of 8 wt% MgO is

Table 2
Primary conditions for MELTS modelling.

Reference database	PRB	A-type granite series	Iceland	SRPY	Cascades
Starting condition wt%	MORB	Average basaltic concentration from most mafic end-member	MORB	MORB	MORB
SiO_2	50.26	42.55	50.26	50.26	50.26
TiO_2	1.36	3.51	1.36	1.36	1.36
Al_2O_3	15.93	17.06	15.93	15.93	15.93
FeO^T	9.34	12.57	9.34	9.34	9.34
MgO	8.00	5.05	8.00	8.00	8.00
CaO	11.64	11.73	11.64	11.64	11.64
Na_2O	2.66	2.96	2.66	2.66	2.66
K_2O	0.10	0.14	0.10	0.10	0.10
P_2O_5	0.13		0.13	0.13	0.13
Starting water content (wt%)	0–4	0–4	0–4	0–4	0–4
Depth/Pressure (kbar)	3	1	1	1	1
Oxygen fugacity (ΔFMQ buffer)	1	0	0	0	1
Co(Th) at MgO = 8 wt%	1.0	3.2	0.7	0.97	0.93
Co(K_2O) at MgO = 8 wt%	1.0	0.5	0.2	0.4	0.67

certainly not a primary mantle-derived magma, it serves as a common starting point for our MELTS modeling and estimation of *F*. Farner and Lee (2017) recognized that the calculated *F* depends on natural variations of C_o, which is controlled by the extent of melting or metasomatism of magma source in the mantle (Turner and Langmuir, 2015), but variations in source conditions are within a factor of 2 or 3, whereas the enrichment in highly evolved (SiO_2 > 70 wt%) arc magmas can exceed a factor of 10. Therefore, our approach is insensitive to source uncertainties for highly evolved magmas, where extreme enrichments have been imparted by extensive crystal fractionation.

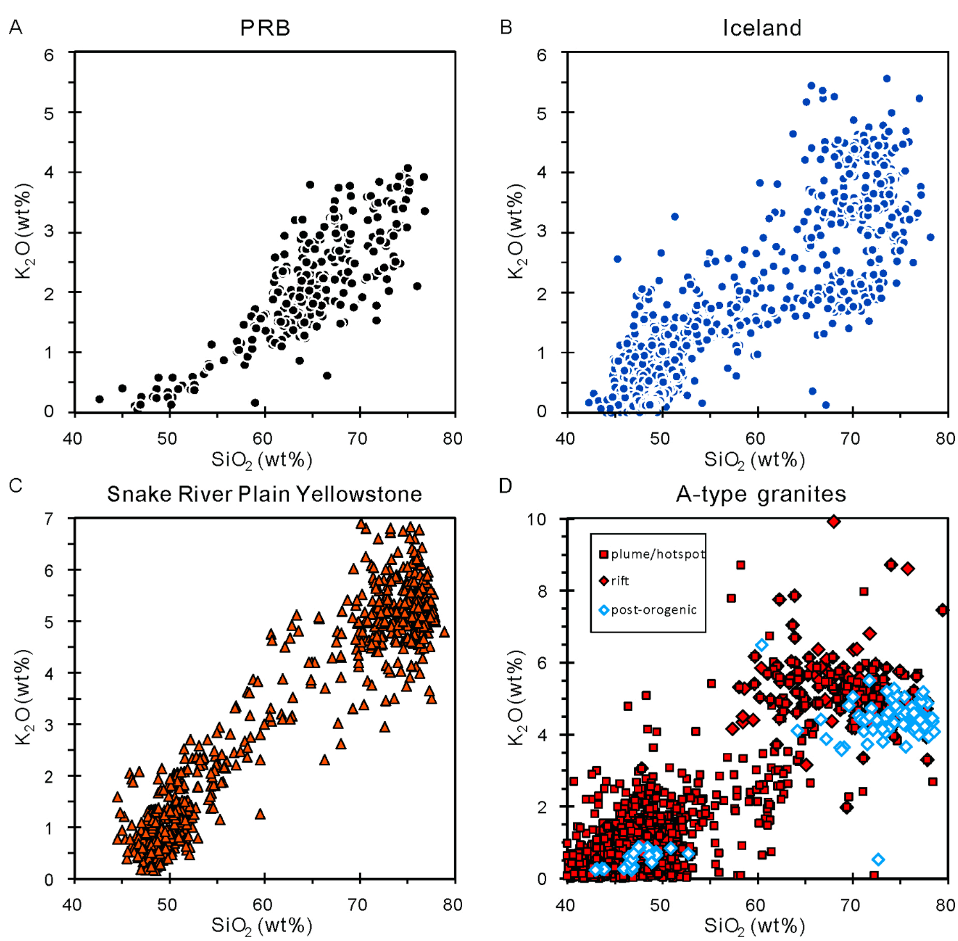

Fig. 1. Bulk rock SiO_2 (wt% on volatile-free basis) versus K_2O (wt%) showing potassium incompatible behavior during magma differentiation for compiled datasets. (A) PRB. (B) Iceland. (C) Snake River Plain Yellowstone. (D) A-type granites.

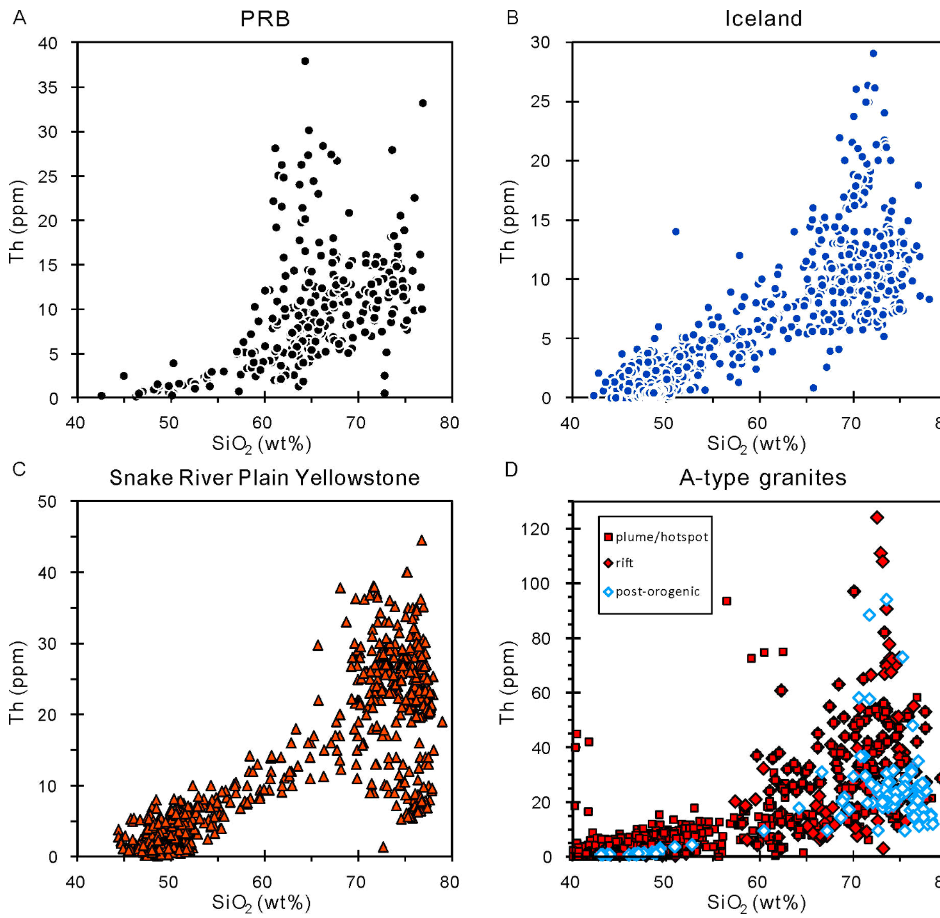

Fig. 2. Diagram of bulk rock SiO_2 (wt% on volatile-free basis) versus Th (ppm) showing the incompatible behavior of thorium. Legends are same as Fig. 1.

3. Modeling results

3.1. Water effect on magmatic evolution

The water content of parental magma plays a fundamental role in determining SiO_2-F variations (Fig. 3), which in turn influences the resultant melt composition produced by magmatic differentiation. Initial magma composition and emplacement depth does not change the modeled curves significantly (Figs. 4 and 5). The most important observation is that the point at which magmas become more silicic is influenced by bulk water content. Under dry conditions, magmas do not increase in SiO_2 until F decreases below ~ 0.2 (Fig. 3A). However, under wet conditions with bulk $H_2O > 2$ wt%, silica increases earlier, beginning at $F \sim 0.6$ (Fig. 3A). In other words, the upwards inflection in SiO_2 of a magma commences earlier in differentiation under water-rich conditions. Thus, water expands the crystallization window over which silicic melts are stable (Fig. 3). This sensitivity of SiO_2-F trends with water content is most pronounced at $H_2O < 2$ wt%. Above 2 wt% H_2O, SiO_2-F trends tend to converge and are no longer sensitive to further changes in bulk H_2O.

Why magmatic water content influences SiO_2-F is related to water's effect on the crystallizing phase assemblage (Berndt et al., 2005; Davenport et al., 2014; Lin et al., 2016; Melekhova et al., 2013; Sisson and Grove, 1993; Zimmer and Plank, 2006). The addition of water into the parental basaltic magma delays crystallization of plagioclase with respect to more mafic phases (pyroxene and olivine), which are lower in silica than plagioclase (Fig. 6A). Therefore, the effect of water is to increase the SiO_2 content of the residual liquid (Fig. 3).

We thus pick up F_{kink} indicated by the F value in terms of the apparent SiO_2 enrichment from modeled magma differentiation curves, which differs as a function of the bulk water content (Fig. 7A). The F_{kink}-H_2O system denotes the water content at the point of most efficient felsic segregation, through which residual melt fraction (F) can be used as a hygrometer for granitoids. Specifically, increasing F_{kink} results in an increase of melt water content. F_{kink} varies from 0.2 at 1 kbar and FMQ 0 to 0.55 over the first 2 wt% H_2O in the melt, and subsequently reaches an apparent plateau value by increasing initial H_2O content of the system (Fig. 7A). The curve is a logarithmic fit to basaltic systems crystallizing under low pressure.

There appears to be some sensitivity of F_{kink} to pressure and oxygen fugacity, but their influences do not change the overall variation trend between F_{kink} and initial H_2O content. Petrological experiments also confirm that water content is the most important factor controlling F (Melekhova et al., 2013). Therefore, we think oxygen fugacity plays a lesser role in controlling F_{kink}, which suggests that F_{kink} can be potentially used as a hygrometer if there are some reasonable bounds on oxygen fugacity (Fig. 8).

3.2. Oxygen fugacity effect

We also explored the effect of oxygen fugacity in controlling magmatic evolution. Oxygen fugacity influences the onset of crystallization of Fe-Ti oxides. In the absence of Fe-Ti oxides, the crystallization of mafic silicate minerals drives MgO downward quickly in the residual magma, such that the Mg# (atomic $Mg^{2+}/(Mg^{2+}+Fe^{2+})$) in the residual magma decreases rapidly with decreasing F or increasing SiO_2. Under oxidizing conditions, Fe-Ti oxide crystallization occurs (Berndt et al., 2005; Zimmer and Plank, 2006), decreasing iron contents in the

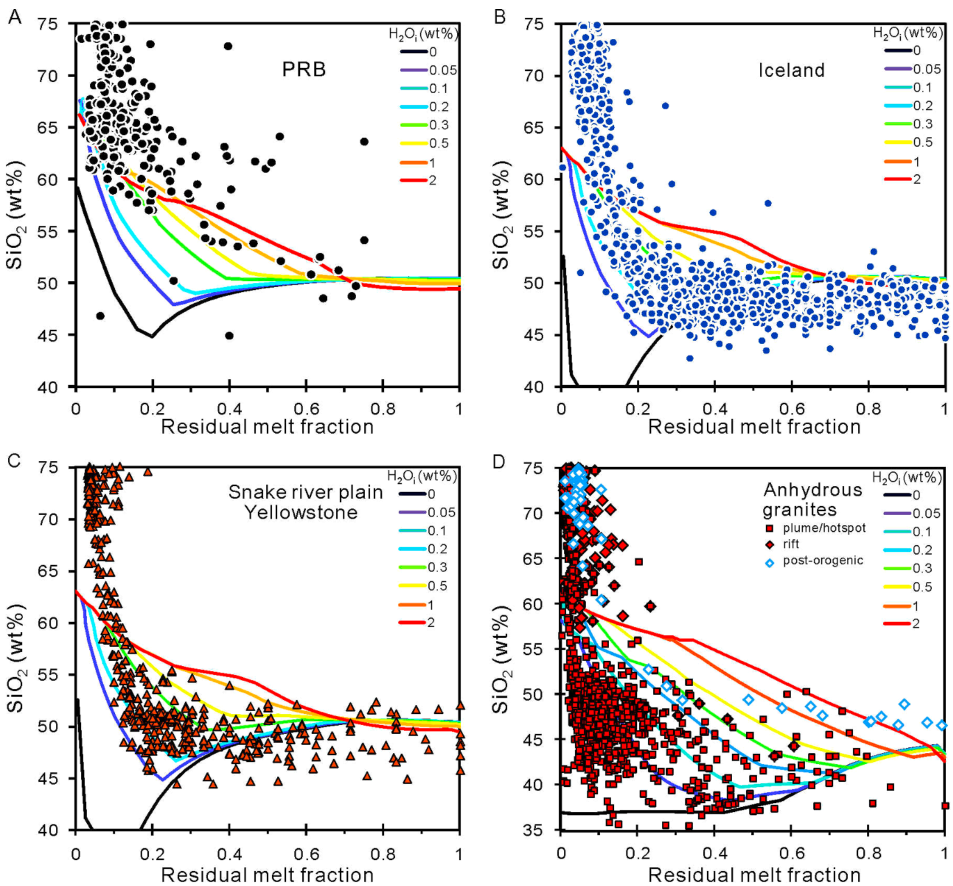

Fig. 3. SiO_2 (wt% on volatile-free basis) versus residual melt fraction F for wet (PRB) and dry (Iceland, SRPY and A type granite series) magmatism. The dotted labels are for compiled natural samples with F calculated using the Th content of the parental basalt assuming Th is perfectly incompatible. Colored curves are Rhyolite-MELTS modeled SiO_2-F results with various water contents. The black lines represent scenarios with initial dry condition, and the colored lines indicate primary water contents up to 4 wt%. (A) Curves are modeled results derived from MORB source at 3 kbar, predicting phase equilibria for magmas with bulk H_2O contents from 0 to 2 wt% (fO_2 at the ΔFMQ buffer). Hydrous granite differentiation trend identified with data from PRB (black circles). (B) Modeled curves of 42 wt% SiO_2 basalt parent at 1 kbar. Suites of magmas (i.e., basalts to rhyolites) of Iceland (blue circles) complied from GEOROC database. (C) Modeled curves from average MORB parent at 1 kbar. Snake River Plain/ Yellowstone (SRPY) rocks are labeled with orange triangles. (D) Anhydrous granite differentiation trend with "A-type granite series" data from different tectonic settings: mantle plume/ hotspot (red squares), rift (red crystals), and post-orogenic settings (blue crystals). Data details can be found in Table 1. (For interpretation of the references to colour in this figure legend, the reader is referred to the web version of this article.)

residual melt and thereby suppressing the decrease in Mg#. In Fig. 6A, it can be seen that the increase in SiO_2 occurs at higher Mg# at high fO_2 conditions compared to that at low fO_2 conditions. We define $Mg\#_{kink}$ as the point at which Mg# stops decreasing and SiO_2 begins to increase. We can see that for oxygen fugacities above the fayalite-magnetite-quartz (ΔFMQ) buffer, $Mg\#_{kink}$ increases with increasing oxygen fugacity due to early magnetite saturation. However, we note that water can also control $Mg\#_{kink}$ (Fig. 7B). This underscores the difficulty of separating the effects of H_2O and fO_2 on magmatic differentiation (Fig. 7B) (Foley, 2011; Kelley and Cottrell, 2009), particularly in the context of Fe, Mg and Mg# as differentiation indices.

4. Applications to nature samples

We now apply the SiO_2-F systematics to natural samples to constrain the initial magma water contents. Compilation of previously published whole-rock major and trace element compositions of two different tectonic settings (arc versus intra-plate) show distinct trends in both SiO_2-F and SiO_2-Mg# systematics (Figs. 3 and 6) Continental arc magmas from PRB show a hydrous and calc-alkaline differentiation trend, while anorogenic/intra-plate magmas mostly follow a dry and tholeiitic differentiation trend (Fig. 6).

4.1. Arc magmatism

As a typical continental arc granitic batholith (Lee et al., 2007), the PRB in southern California defines a magmatic differentiation clearly above the trends of intra-plate magmas in the SiO_2-Mg# system (Fig. 6). Their Mg# first deceases to 0.5 before SiO_2 increases to 50 wt% and then maintains a relatively high Mg# until SiO_2 reaches 70 wt%, after which Mg# shows a rapid decline with further differentiation. The high Mg# of PRB magmas reflects the Fe depletion during calc-alkaline differentiation. Fe depletion can be driven by magnetite fractionation under oxidized conditions (Berndt et al., 2005). Alternatively, garnet fractionation at high pressure, which may also scavenge Fe from the melt (Alonso-Perez et al., 2008; Green and Ringwood, 1968; Tang et al., 2018), which mechanism plays the dominant role is contentious. But this debate is not important for our discussions of water effect on SiO_2 enrichment here, because both magnetite and garnet have little to low SiO_2 contents, and are favored under hydrous conditions (Alonso-Perez et al., 2008; Green and Ringwood, 1968; Zimmer et al., 2010), and their fractionation would increase SiO_2 content of the derivative melt. It is noteworthy that the continental crust compositions roughly fall on the PRB Mg#-SiO_2 trend (Fig. 6B), indicating that the continental crust was predominantly formed under hydrous conditions comparable to those of arc magmatism. In the SiO_2-F diagram (Fig. 3A), PRB samples show a rapid increase in SiO_2 content as F reduces to ~0.6. Using F_{kink} = 0.6 in our hygrometer (Fig. 7A) gives an initial magma water content > 2 wt %.

The Cascades arc volcanism in western North America was thought to be related with slab dehydration before the magmatic arc front (Syracuse et al., 2010), and they show similar results (Fig. 9) as the PRB rocks, corroborating our argument that water impacts the SiO_2-F relationship during magma differentiation. Our hygrometer application with F_{kink} = 0.6 shows primary wet water conditions with initial H_2O > 2 wt% for them.

4.2. Intra-plate magmatism

Intra-plate magmatic rocks display SiO_2-Mg# and SiO_2-F systematics different from those of arc magmas. Mg# decreases rapidly with differentiation in intra-plate samples, generating low Mg# felsic rocks

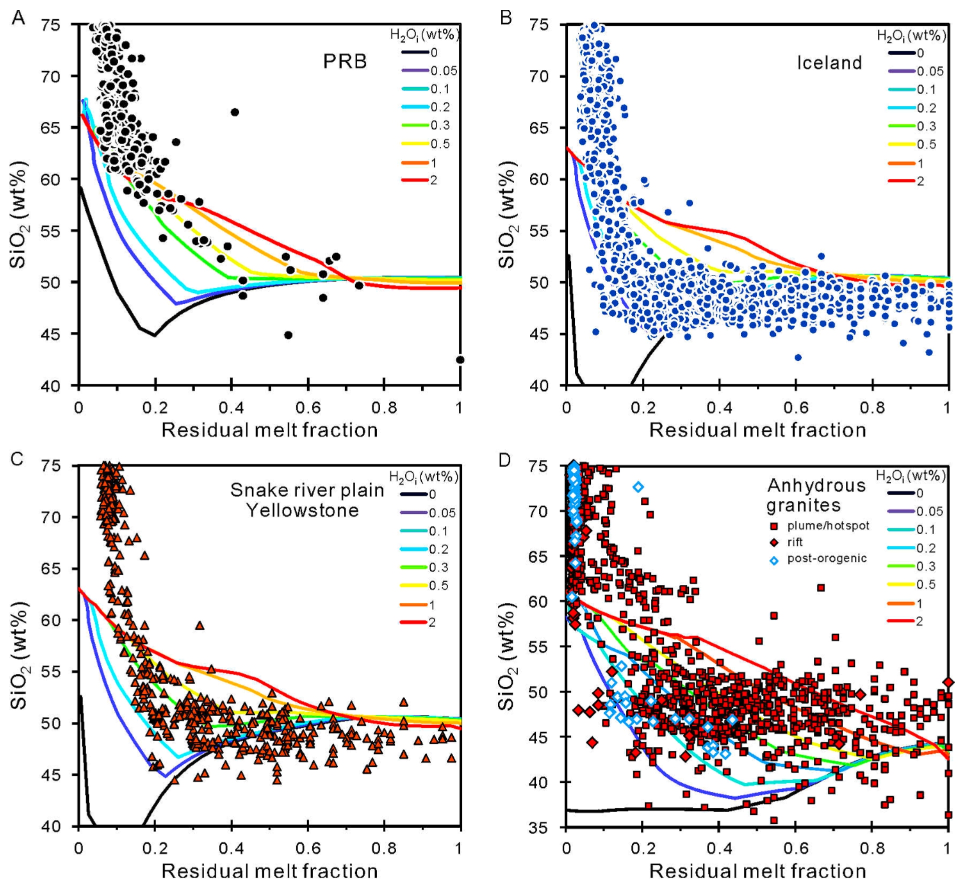

Fig. 4. SiO_2 (wt% on volatile-free basis) versus residual melt fraction *F* calculated based on bulk-rock K_2O concentration. This diagram shows similar trend with Fig. 3.

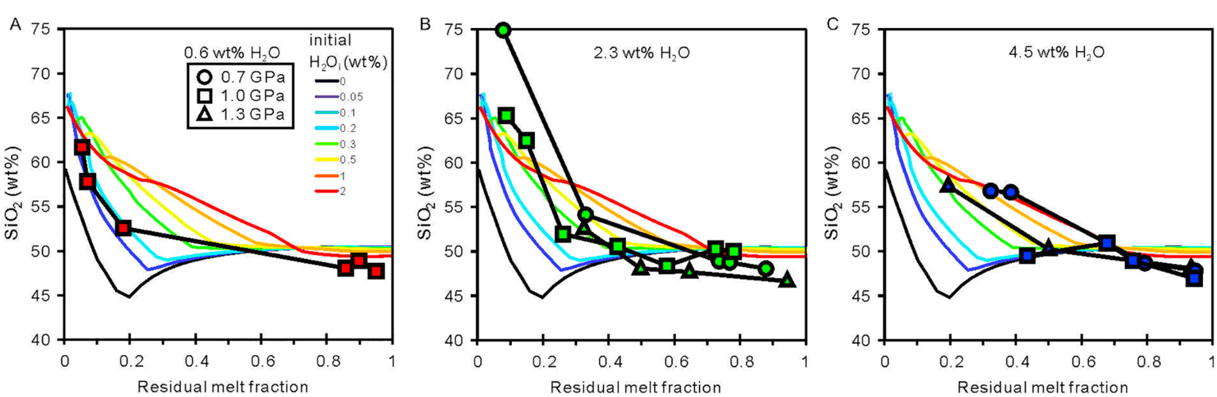

Fig. 5. Compiled experimental data from Melekhova et al. (2013) showing the effect of primary water content on SiO_2-*F* magma differentiation trend. Water increase of the crystallization system corresponds to higher *F* values when SiO_2 start to increase. Depth is not the critical factor that changes the differentiation trend.

(Fig. 6D). The SiO_2-*F* systematics indicates dry differentiation of most intra-plate magmas, consistent with experimental results (Maaløe and Wyllie, 1975). SiO_2 remains low and nearly constant with differentiation, only rises after *F* decreases to 0.2 (Fig. 6B–D). As a consequence, in intra-plate settings, felsic magmas can only be generated by extreme differentiation ($F < 0.2$). For both Iceland and Snake River Plain Yellowstone (SRPY), F_{kink} occurs at ~0.2. Using this F_{kink} in our hygrometer (Fig. 7A) yields initial water content < 0.5 wt% (Fig. 3).

It is noted that there is a small fraction of the data, particularly for post-orogenic A2-type granites, showing extreme high Mg# between 0.25 and 0.5. This indicates that the water contents of some A2-type granites are different from the common A1-type rocks (Anderson et al., 2003; Auwera et al., 2003; Bonin, 2007; Clemens et al., 1986; Eby, 1992; Frost and Frost, 1997, 2011; Hannah and Stein, 1986; Turner et al., 1992) since they form immediately after orogenesis and can inherit the similar water content as orogeny-related granitoids (Fig. 6D). This is also consistent with the SiO_2-*F* plot that post-orogenic granitic rocks have high water content relatively to A1-type granites. We suggest that the high Mg# of A2-type granites in Fig. 6D may result from extreme differentiation.

4.3. Implications for Archean TTGs

Archean TTGs show a silica versus Mg# trend similar to that of arc

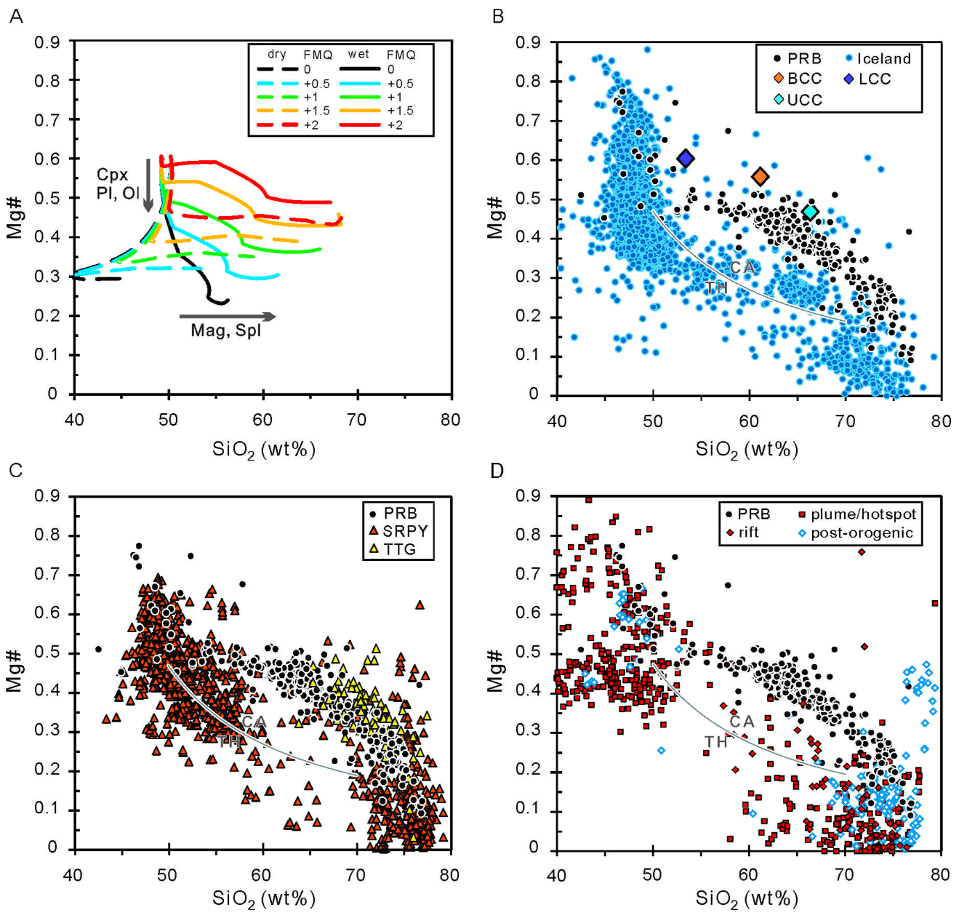

Fig. 6. Whole-rock Mg# (molar $Mg^{2+}/(Mg^{2+}+Fe^{2+})$) versus SiO_2 (wt% on volatile-free basis) diagrams showing continuous differentiation trends linking the mafic to the felsic end-member for hydrous and anhydrous granites respectively. A: Rhyolite-MELTS modeled results from MORB source with distinct primary water content and oxygen fugacity. The solid lines indicate wet (2 wt%) condition, while the dashed lines represent dry conditions. Lines with different colors represent scenarios under different oxygen fugacities, with ΔFMQ buffer from 0 to +2. For dry magmas, all calculated curves show Mg# drop at SiO_2 around 50 wt% before water saturation, indicating Cpx (clinopyroxene) and Pl (plagioclase) crystallization which leads to the decrease of Mg#, and SiO_2 increase after that with low Mg#, which is due to the crystallization of Mag (Magnetite) and Spl (Spinel) after water saturation. While modeled differentiation for wet magmas at high fO_2 increasing SiO_2 with early crystallization of Mag and Spl at Mg# around 50 wt%, and later slight Mg# decrease at SiO_2 around 55 wt% because of water saturation. B-D: Legends are same with Fig. 1. Lower, bulk and upper continental crust are identified big crystals (purple, orange and blue) respectively with data from Rudnick and Gao (2004). Archean TTG (yellow triangles) data are from GEOROC. The grey solid line represents revised TH (tholeiitic)-CA(calc-alkaline) boundary from Miyashiro (1974). (For interpretation of the references to colour in this figure legend, the reader is referred to the web version of this article.)

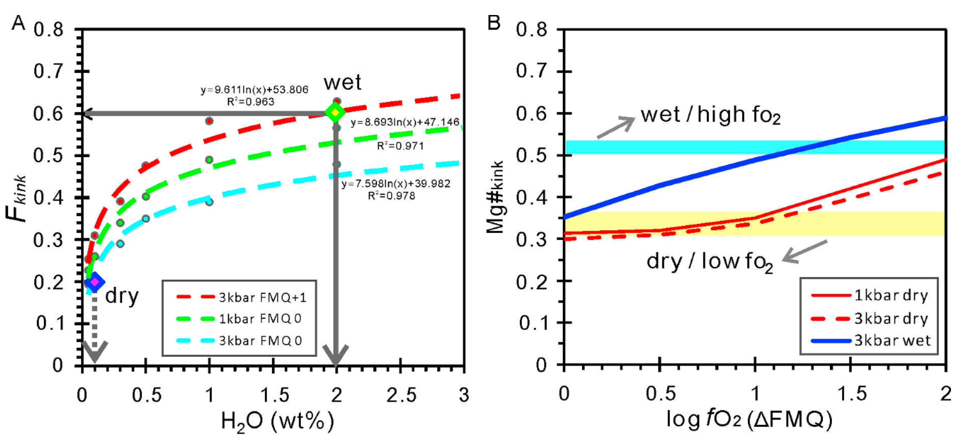

Fig. 7. A: Residual melt fraction (F) as a function of bulk system water contents (H_2O) based on Rhyolite-MELTS (Gualda and Ghiorso, 2015) calculation with MORB parental magma. Dashed lines are colored for different pressures ranging from 1 to 3 kbar, and log fO_2 from ΔFMQ 0 to +1. Grey solid arrows indicate that for the arc magmatism cooling at 3kbar and ΔFMQ + 1, medium-high silicic differentiation starts at F_{kink} of 0.6, corresponding to water content of 2 wt%, while grey dotted arrow represents F_{kink} for dry granite corresponds to initial H_2O content of 0.1 wt%. B: The kink of whole rock Mg# sudden increase as a function of oxygen fugacity. $Mg\#_{kink}$ (Mg# value with the onset of magnetite crystallization) can be used as a proxy of fO_2 with the observed positive relationship. Blue and yellow shaded boxes show the range proposed for $Mg\#_{kink}$ of arc and intra-plate magmatism, respectively. The light blue bar reflects the high fO_2 corresponding to magnetite crystallization at higher Mg#, while the yellow bar indicates late magnetite crystallization at lower Mg#. Besides, the solid blue and red curves show that increase of water content also increases the $Mg\#_{kink}$. The influence of emplacing depth is not obviously observed from the solid and dashed red curves. (For interpretation of the references to colour in this figure legend, the reader is referred to the web version of this article.)

magmas and also imply high fO_2 and H_2O (Fig. 6C). This similarity does not necessarily indicate the initiation of plate tectonics at Early Archean time, but in fact suggests the important role of water in the formation of Archean TTGs. Dry intra-plate tectonic settings may not be feasible for water circulation in the whole crust and between the mantle and crust. Therefore, plume-related magmatism may not be the dominant factor in the evolution of Early Archean continental crust.

5. Conclusions

This study highlights the role of water in generating silicic magmas, which promotes early SiO_2 enrichment in the melt. The SiO_2-F systematics can be a potentially powerful hygrometer to quantify initial magma water contents. Application of this hygrometer to natural samples shows that Phanerozoic arc felsic rocks and Archean TTGs were

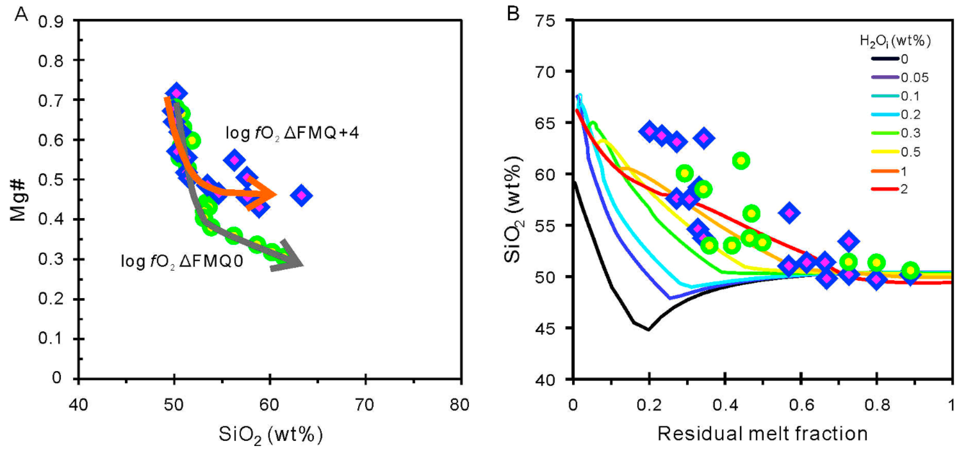

Fig. 8. Compiled experimental data from Berndt et al. (2005) showing the effect of oxygen fugacity on magma evolution. (A) Oxygen fugacity plays important role in magma differentiation trend of SiO_2-Mg# systematics. (B) SiO_2-F trend is not affected by the factor of oxygen fugacity.

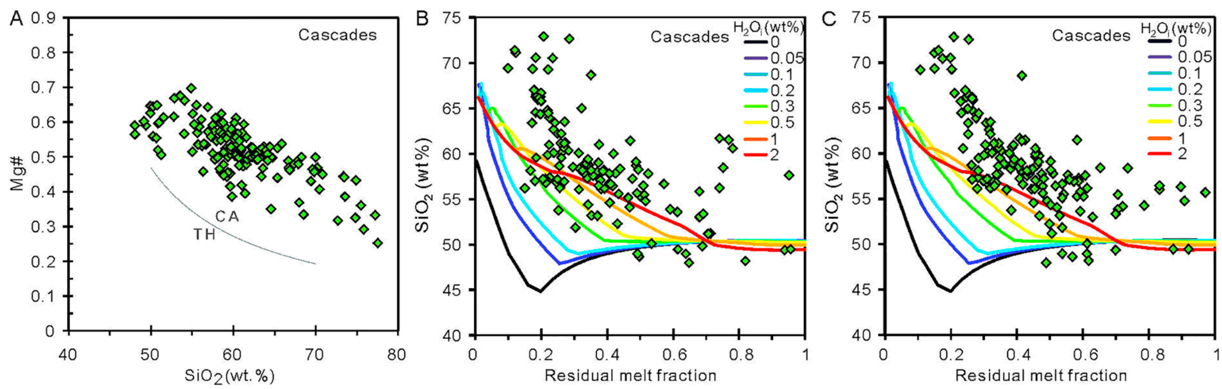

Fig. 9. Diagrams of magma differentiation of Cascades volcanic rocks in western North America showing similar behavior with PRB-like arc magmatism. Data of the Cascades volcanic rocks are from GEOROC. The grey solid line represents revised TH (tholeiitic) - CA(calc-alkaline) boundary of Miyashiro (1974).

formed by hydrous differentiation, whereas intra-plate silicic magmas and A1-type granites mostly differentiated under dry conditions.

Conflict of interest

The authors declared that there is no conflict of interest.

Acknowledgments

This work was supported by the National Key R&D Project of China (grant number 2016YFC0600203); the National Natural Science Foundation of China (grant number 41472049). The author X. Chen is grateful for the financial support from China Scholarship Council and Program B for Outstanding PhD candidate of Nanjing University. The manuscript benefits discussions with Prof. Y.F. Zheng.

References

Alonso-Perez, R., Müntener, O., Ulmer, P., 2008. Igneous garnet and amphibole fractionation in the roots of island arcs: experimental constraints on andesitic liquids. Contrib. Mineral. Petrol. 157 (4), 541.
Anderson, I.C., Frost, C.D., Frost, B.R., 2003. Petrogenesis of the Red Mountain pluton, Laramie anorthosite complex, Wyoming: implications for the origin of A-type granite. Precambrian Res. 124 (2), 243–267.
Ague, J.J., Brimhall, G.H., 1988. Magmatic arc asymmetry and distribution of anomalous plutonic belts in the batholiths of California: effects of assimilation, crustal thickness, and depth of crystallization. Bull. Geol. Soc. Am. 100, 912–927.
Annen, C., Blundy, J.D., Sparks, R.S.J., 2006. The genesis of intermediate and silicic magmas in deep crustal hot zones. J. Petrol. 47, 505–539.
Asimow, P.D., Langmuir, C.H., 2003. The importance of water to oceanic mantle melting regimes. Nature 421 (6925), 815–820.
Auwera, J.V., Bogaerts, M., Liégeois, J.P., Demaiffe, D., Wilmart, E., Bolle, O., Duchesne, J.C., 2003. Derivation of the 1.0-0.9 Ga ferro-potassic A-type granitoids of southern Norway by extreme differentiation from basic magmas. Precambrian Res. 124 (2), 107–148.
Berndt, J., Koepke, J., Holtz, F., 2005. An experimental investigation of the influence of water and oxygen fugacity on differentiation of MORB at 200 MPa. J. Petrol. 46 (1), 135–167.
Bonin, B., 2007. A-type granites and related rocks: evolution of a concept, problems and prospects. Lithos 97 (1), 1–29.
Bonin, B., Grelou-Orsini, C., Vialette, Y., 1978. Age, origin and evolution of the anorogenic complex of Evisa (Corsica): a K-Li-Rb-Sr study. Contrib. Mineral. Petrol. 65 (4), 425–432.
Campbell, I., Taylor, S., 1983. No water, no granites - no oceans, no continents. Geophys. Res. Lett. 10 (11), 1061–1064.
Clemens, J.D., Holloway, J.R., White, A.J.R., 1986. Origin of an A-type granite; experimental constraints. Am. Mineral. 71 (3), 317–324.
Capaldi, G., Chiesa, S., Manetti, P., Orsi, G., Poli, G., 1987. Tertiary anorogenic granites of the western border of the Yemen Plateau. Lithos 20 (6), 433–444.
Collins, W., Beams, S., White, A., Chappell, B., 1982. Nature and origin of A-type granites with particular reference to southeastern Australia. Contrib. Mineral. Petrol. 80 (2), 189–200.
Condie, K.C., 2013. Plate Tectonics and Crustal Evolution. Elsevier.
Davenport, J.D., Longhi, J., Neal, C.R., Bolster, D., Jolliff, B.L., 2014. Simulating planetary igneous crystallization environments (SPICEs): a suite of igneous crystallization programs. In: Proceedings Lunar and Planetary Science Conference 2014, pp. 1111.
Dong, Y., Zhang, G., Neubauer, F., Liu, X., Hauzenberger, C., Zhou, D., Li, W., 2011. Syn- and post-collisional granitoids in the Central Tianshan orogen: Geochemistry, geochronology and implications for tectonic evolution. Gondwana Res. 20 (2), 568–581.
Eby, G.N., 1990. The A-type granitoids: a review of their occurrence and chemical characteristics and speculations on their petrogenesis. Lithos 26 (1), 115–134.
Eby, G.N., 1992. Chemical subdivision of the A-type granitoid: petrogenetic and tectonic implication. Geology 20 (7), 641.
Eby, G.N., Krueger, H.W., Creasy, J.W., 1992. Geology, geochronology, and geochemistry of the White Mountain batholith, New Hampshire. Geol. Soc. Am. Special Papers 268, 379–398.
Farner, M.J., Lee, C.T.A., 2017. Effects of crustal thickness on magmatic differentiation in subduction zone volcanism: a global study. Earth Planet. Sci. Lett. 470, 96–107.
Fletcher, C., Beddoe-Stephens, B., 1987. The petrology, chemistry and crystallization history of the Velasco alkaline province, eastern Bolivia. Geol. Soc., London, Special

Publ. 30 (1), 403–413.
Foley, S.F., 2011. A reappraisal of redox melting in the earth's mantle as a function of tectonic setting and time. J. Petrol. 52 (7–8), 1363–1391.
Frost, C.D., Frost, B.R., 1997. Reduced rapakivi-type granites: the tholeiite connection. Geology 25 (7), 647.
Frost, C.D., Frost, B.R., 2011. On Ferroan (A-type) granitoids: their compositional variability and modes of origin. J. Petrol. 52 (1), 39–53.
Glazner, A.F., Johnson, B.R., 2013. Late crystallization of K-feldspar and the paradox of megacrystic granites. Contrib. Mineral. Petrol. 166 (3), 777–799.
Green, T.H., Ringwood, A.E., 1968. Origin of garnet phenocrysts in calc-alkaline rocks. Contrib. Mineral. Petrol. 18 (2), 163–174.
Gualda, G.A., Ghiorso, M.S., 2015. MELTS_Excel: A Microsoft Excel-based MELTS interface for research and teaching of magma properties and evolution. Geochem., Geophys., Geosyst. 16 (1), 315–324.
Hannah, J.L., Stein, H.J., 1986. Oxygen isotope compositions of selected laramide-tertiary granitoid stocks in the Colorado Mineral Belt and their bearing on the origin of climax-type granite-molybdenum systems. Contrib. Mineral. Petrol. 93 (3), 347–358.
Holm, P.M., Prægel, N.O., 1988. The Tertiary Kærven Syenite Complex, Kangerdlugssuaq, East Greenland: mineral chemistry and geochemistry. Mineral. Mag. 52, 435–450.
Jiang, N., Guo, J., Zhai, M., 2011. Nature and origin of the Wenquan granite: implications for the provenance of Proterozoic A-type granites in the North China craton. J. Asian Earth Sci. 42 (1), 76–82.
Katz, R.F., Spiegelman, M., Langmuir, C.H., 2003. A new parameterization of hydrous mantle melting. Geochemistry, Geophysics, Geosystems 4, 9.
Kelley, K.A., Cottrell, E., 2009. Water and the oxidation state of subduction zone magmas. Science 325 (5940), 605–607.
Kushiro, I., 1972. Effect of water on the composition of magmas formed at high pressures. J. Petrol. 13 (2), 311–334.
Leat, P., Jackson, S., Thorpe, R., Stillman, C., 1986. Geochemistry of bimodal basalt-subalkaline/peralkaline rhyolite provinces within the Southern British Caledonides. J. Geol. Soc. 143 (2), 259–273.
Lee, C.T.A., Bachmann, O., 2014. How important is the role of crystal fractionation in making intermediate magmas? Insights from Zr and P systematics. Earth Planet. Sci. Lett. 393, 266–274.
Lee, C.T.A., MorTon, D.M., Farner, M.J., MoiTrA, P., 2015. Field and model constraints on silicic melt segregation by compaction/hindered settling: the role of water and its effect on latent heat release. Am. Mineral. 100 (8–9), 1762–1777.
Lee, C.T.A., Morton, D.M., Kistler, R.W., Baird, A.K., 2007. Petrology and tectonics of Phanerozoic continent formation: from island arcs to accretion and continental arc magmatism. Earth Planet. Sci. Lett. 263 (3), 370–387.
Lin, Y.H., Tronche, E.J., Steenstra, E.S., Westrenen, W.V., 2016. Evidence for an early wet Moon from experimental crystallization of the lunar magma ocean. Nature Geosci. 10, 1.
Maaløe, S., Wyllie, P.J., 1975. Water content of a granite magma deduced from the sequence of crystallization determined experimentally with water-undersaturated conditions. Contribut. Mineral. Petrol. 52 (3), 175–191.
Macdonald, R., Davies, G., Bliss, C., Leat, P., Bailey, D., Smith, R., 1987. Geochemistry of high-silica peralkaline rhyolites, Naivasha, Kenya Rift Valley. J. Petrol. 28 (6), 979–1008.
Melekhova, E., Annen, C., Blundy, J., 2013. Compositional gaps in igneous rock suites controlled by magma system heat and water content. Nat. Geosci. 6 (5), 385–390.
Miyashiro, A., 1974. Volcanic rock series in island arcs and active continental margins. Am. J. Sci. 274 (4), 321–355.
Nelson, D.O., Nelson, K.L., Reeves, K.D., Mattison, G.D., 1987. Geochemistry of Tertiary alkaline rocks of the eastern Trans-Pecos magmatic province, Texas. Contrib. Mineral. Petrol. 97 (1), 72–92.
Nutman, A.P., 2006. Comment on "Zircon thermometer reveals minimum melting conditions on earliest Earth" II. Science 311 (5762) 779b–779b.
Qu, X.M., Wang, R.J., Xin, H.B., Jiang, J.H., Chen, H., 2012. Age and petrogenesis of A-type granites in the middle segment of the Bangonghu-Nujiang suture, Tibetan plateau. Lithos 146, 264–275.
Rämö, O.T., 1991. Petrogenesis of the Proterozoic rapakivi granites and related basic rocks of southeastern Fennoscandia: Nd and Pb isotopic and general geochemical constraints. Geologian tutkimuskeskus.
Rollinson, H.R., 2014. Using Geochemical Data: Evaluation, Presentation, Interpretation. Routledge.
Rudnick, R.L., Gao, S., 2004. Composition of the continental crust. In: Rudnick, R.L., Holland, H.D., Turekian, K.K. (Eds.), The Crust, Treatise on Geochemistry 3. Elsevier-Pergaman, Oxford, pp. 1–64.
Shaw, D.M., 1970. Trace element fractionation during anatexis. Geochim. Cosmochim. Acta 34 (2), 237–243.
Sisson, T.W., Grove, T.L., 1993. Experimental investigations of the role of H_2O in calc-alkaline differentiation and subduction zone magmatism. Contrib. Mineral. Petrol. 113, 143–166.
Sizova, E., Gerya, T., Stüwe, K., Brown, M., 2015. Generation of felsic crust in the Archean: a geodynamic modeling perspective. Precambrian Res. 271, 198–224.
Syracuse, E.M., van Keken, P.E., Abers, G.A., 2010. The global range of subduction zone thermal models. Phys. Earth Planet. Interiors 183 (1), 73–90.
Tang, M., Chen, K., Robert, R., 2016. Archean upper crust transition from mafic to felsic marks the onset of plate tectonics. Science 351, 372–375.
Tang, M., Erdman, M., Eldridge, G., Lee, C.T.A., 2018. The redox "filter" beneath magmatic orogens and the formation of continental crust. Sci. Adv. 4, 5.
Turner, S.J., Langmuir, C.H., 2015. What processes control the chemical compositions of arc front stratovolcanoes? Geochem., Geophys., Geosyst. 16 (6), 1865–1893.
Turner, S.P., Foden, J.D., Morrison, R.S., 1992. Derivation of some A-type magmas by fractionation of basaltic magma: an example from the Padthaway Ridge, South Australia. Lithos 28 (2), 151–179.
Valley, J.W., Cavosie, A.J., Ushikubo, T., Reinhard, D.A., Lawrence, D.F., Larson, D.J., Clifton, P.H., Kelly, T.F., Wilde, S.A., Moser, D.E., Spicuzza, M.J., 2014. Hadean age for a post-magma-ocean zircon confirmed by atom-probe tomography. Nat. Geosci. 7, 219–223.
Watson, E., Harrison, T., 2005. Zircon thermometer reveals minimum melting conditions on earliest Earth. Science 308 (5723), 841–844.
Weller, O.M., St-Onge, M.R., 2017. Record of modern-style plate tectonics in the Paleoproterozoic Trans-Hudson orogen. Nat. Geosci. 10, 305–311.
Whitney, J.A., 1988. The origin of granite: the role and source of water in the evolution of granitic magmas. Geol. Soc. Am. Bull. 100 (12), 1886–1897.
Wolf, M.B., Wyllie, P.J., 1994. Dehydration-melting of amphibolite at 10kb: the effects of temperature and time. Contrib. Mineral. Petrol. 115, 369–383.
Woolley, A., Jones, G., 1987. The petrochemistry of the northern part of the Chilwa alkaline province, Malawi. Geol. Soc., London, Special Publ. 30 (1), 335–355.
Wormald, R., Price, R., 1988. Peralkaline granites near Temora, southern New South Wales: tectonic and petrological implications. J. Geol. Soc. Australia 35 (2), 209–221.
Zhao, T.P., Zhou, M.F., 2009. Geochemical constraints on the tectonic setting of Paleoproterozoic A-type granites in the southern margin of the North China Craton. J. Asian Earth Sci. 36 (2), 183–195.
Zhao, X.F., Zhou, M.F., Li, J.W., Wu, F.Y., 2008. Association of Neoproterozoic A-and I-type granites in South China: implications for generation of A-type granites in a subduction-related environment. Chem. Geol. 257 (1), 1–15.
Zhong, H., Zhu, W.G., Chu, Z.Y., He, D.F., Song, X.Y., 2007. SHRIMP U-Pb zircon geochronology, geochemistry, and Nd-Sr isotopic study of contrasting granites in the Emeishan large igneous province SW China. Chem. Geol. 236 (1), 112–133.
Zhu, W.G., Zhong, H., Li, X.H., He, D.F., Song, X.Y., Ren, T., Chen, Z.Q., Sun, H.S., Liao, J.Q., 2010. The early Jurassic mafic-ultramafic intrusion and A-type granite from northeastern Guangdong, SE China: age, origin, and tectonic significance. Lithos 119 (3), 313–329.
Zimmer, M., Plank, T., 2006. The role of water in generating Fe-depletion and the calc-alkaline trend. In: AGU Fall Meeting Abstracts 1, 0636.
Zimmer, M.M., Plank, T., Hauri, E.H., Yogodzinski, G.M., Stelling, P., Larsen, J., Singer, B., Jicha, B., Mandeville, C., Nye, C.J., 2010. The role of water in generating the calc-alkaline trend: new volatile data for aleutian magmas and a new tholeiitic index. J. Petrol. 51 (12), 2411–2444.